H2 in solid C60: Coupled translation-rotation eigenstates in the octahedral interstitial site from quantum five-dimensional calculations

Shufeng Ye, Minzhong Xu, Stephen FitzGerald, Kirill Tchernyshyov, and Zlatko Bai

Citation: The Journal of Chemical Physics **138**, 244707 (2013); doi: 10.1063/1.4811220
View online: http://dx.doi.org/10.1063/1.4811220
View Table of Contents: http://scitation.aip.org/content/aip/journal/jcp/138/24?ver=pdfcov
Published by the AIP Publishing

H_2 in solid C_{60}: Coupled translation-rotation eigenstates in the octahedral interstitial site from quantum five-dimensional calculations

Shufeng Ye,[1] Minzhong Xu,[1] Stephen FitzGerald,[2] Kirill Tchernyshyov,[2] and Zlatko Bačić[1,a)]
[1]*Department of Chemistry, New York University, New York, New York 10003, USA*
[2]*Department of Physics and Astronomy, Oberlin College, Oberlin, Ohio 44074, USA*

(Received 30 April 2013; accepted 3 June 2013; published online 27 June 2013)

We report rigorous quantum five-dimensional (5D) calculations of the coupled translation-rotation (TR) energy levels and wave functions of an H_2 molecule, in the ground ($v = 0$) and vibrationally excited ($v = 1$) states, confined inside the octahedral interstitial site of solid C_{60} with S_6 symmetry. Translational and rotational excitations of H_2 in this nanocavity have been measured by the inelastic neutron scattering (INS) and infrared (IR) spectroscopy, enabling direct comparison between theory and experiment. A pairwise additive 5D intermolecular potential energy surface (PES) was employed in the calculations. The quantum calculations cover the range of energies and types of translational and rotational excitations of the guest molecule which go substantially beyond those considered in the earlier theoretical investigations of this system, revealing new information about the TR energy level structure. The computed $j = 1$ and $j = 2$ rotational levels and their splittings, as well as the translational fundamental, are in semi-quantitative agreement with the available INS and IR data, indicating the need for a more accurate intermolecular PES. Our calculations reveal a strong dependence of the TR energy levels, in particular their splittings, on the setting angle which defines the orientation of the C_{60} molecules relative to their local threefold axes. © *2013 AIP Publishing LLC*. [http://dx.doi.org/10.1063/1.4811220]

I. INTRODUCTION

Entrapment of hydrogen molecules inside nanoscale cavities of host materials has received considerable attention in recent years, from experimentalists and theorists alike. Its relevance for hydrogen storage applications has been the main driving force behind much of the research aimed at molecular hydrogen in clathrate hydrates[1–5] and metal-organic frameworks (MOFs).[6–9] Endohedral fullerene complexes encapsulating the H_2 molecule, because of their low weight percentage of hydrogen, are unlikely candidates for hydrogen storage applications. Nevertheless, a great deal of experimental research has been directed at H_2 inside the C_{60} molecule ($H_2@C_{60}$) and aza-thia-open-cage fullerene (ATOCF),[10–19] to gain understanding of the dynamics of the nanoconfined H_2 molecule. These spectroscopic investigations have been complemented by the rigorous theoretical treatments of the quantum dynamics of H_2 in C_{60},[20–22] C_{70},[22,23] and ATOCF.[24]

Confinement of the H_2 molecule results in the quantization of the three translational degrees of freedom of its center of mass (cm). The discrete translational eigenstates are well separated in energy because of the small mass of the H_2 and the tightness of the confining cavity. The same holds for the quantized rotational levels of H_2 owing to its exceptionally large rotational constant. The resulting coupled translation-rotation (TR) energy level structure is sparse. It is even sparser because of the symmetry constraints on the total wave function of H_2 (and D_2), which lead to the existence of two distinct species, *para*-H_2 (p-H_2) which has only even-j rotational states ($j = 0, 2, \ldots$), and *ortho*-H_2 (o-H_2) with odd-j rotational states only ($j = 1, 3, \ldots$). Consequently, the TR dynamics of the encapsulated H_2 is highly quantum mechanical, especially at the low temperatures at which most of the spectroscopic measurements are performed.

The quantum TR dynamics of the trapped H_2 molecule is strongly influenced by the symmetry of the confining nanocage, which leaves clear fingerprints in the patterns of the degeneracies of the TR energy levels and their splittings, the types of quantum numbers appropriate for the assignment of the translational excitations, and the nature of coupling between the angular momenta associated with the translational and rotational motions, respectively. This was brought to light and analyzed in our systematic studies of the quantum five-dimensional (5D) TR dynamics and eigenstates of H_2 inside fullerenes of decreasing symmetry, C_{60} (I_h),[20–22] C_{70} (D_{5h}),[22,23] and ATOCF (C_1).[24]

This line of investigation has lead us to consider the quantum TR dynamics of H_2 confined inside the interstitial cavities of solid C_{60}. The centers of the C_{60} molecules form an fcc lattice. For temperatures above about 260 K, the C_{60} molecules are orientationally disordered, rotate rather freely. At 260 K a phase transition occurs to the low-temperature structure which is orientationally ordered and has the $Pa\bar{3}$ crystal symmetry.[25–27] It has been well established that H_2 singly occupies the octahedral interstitial sites of solid C_{60}. In the orientationally disordered phase, above 260 K, the octahedral site has O_h symmetry. Below this temperature, the orientational ordering lowers the local symmetry of the octahedral interstitial site to that of the point group S_6.[11,28] Since the neighboring octahedral sites are well separated, the

a)Electronic mail: zlatko.bacic@nyu.edu

interaction between the H_2 molecules occupying them is negligible. Consequently, the system can be treated as an isolated H_2 molecule inside the octahedral interstitial cavity.

The quantum TR dynamics of interstitial H_2 in solid C_{60} has been probed experimentally using inelastic neutron scattering (INS),[28] NMR,[11,29] infrared (IR) spectroscopy,[30,31] and Raman spectroscopy.[32] It has also been the subject of several theoretical studies.[28,33,34] Moreover, the diffusion of H_2 in solid C_{60} has been investigated both theoretically[35] and experimentally.[36] Despite considerable experimental and theoretical efforts, quantitative understanding of the quantum TR dynamics of H_2 in the octahedral site is still lacking. The experimental data regarding the TR excitations are rather limited and insufficiently resolved. The theoretical studies[33,34] have provided valuable insights into the TR dynamics, but the definitive interpretation of the measured spectra has not been achieved. This is in part due to the deficiencies of the existing potentials for the interaction of H_2 with the C_{60} molecules forming the octahedral site. In addition, these theoretical treatments have employed various decoupling approximations aimed at reducing the dimensionality of the quantum dynamics treatment, which introduce uncertainties in the results and the conclusions based on them. There has been no fully coupled quantum 5D calculation of the TR eigenstates of H_2 in the octahedral cavity.

This has motivated us to undertake the theoretical study whose results are reported in this paper. We have performed rigorous quantum 5D calculations of the TR energy levels and wave functions of an H_2 molecule in the octahedral interstitial site of solid C_{60}, for both the ground ($\nu = 0$) and the vibrationally excited ($\nu = 1$) states of the guest molecule. The translational and rotational degrees of freedom of H_2 are treated as fully coupled, without invoking any reduced-dimensionality approximations. A pairwise additive intermolecular potential energy surface (PES) was employed, which was used in several earlier studies of this system.[11,28,33] Our results are numerically exact for the PES employed, and constitute a benchmark with which other theoretical approaches can be compared. The TR eigenstates characterized in the present work span the range of energies and types of translational and rotational excitations which go well beyond those probed in the previous theoretical investigations, leading to new and interesting insights. Extensive comparison is made with the existing spectroscopic data and the results of earlier theoretical studies. In the next stage of the investigations, already under way in our group, the 5D coupled TR wave functions obtained in the present study will serve as an input for the quantum simulation of the INS spectra of H_2 in solid C_{60}, using the methodology recently developed by us, which allows rigorous calculations of the INS spectra of a hydrogen molecule inside a nanoscale cavity.[37–39]

II. THEORETICAL METHODOLOGY

A. Potential energy surface for H_2 in the octahedral interstitial site

We consider solid C_{60} having the orientationally ordered low-temperature structure with the overall $Pa\bar{3}$ crystal symmetry, and C_{60} molecules in the "major" (or p), orientation.[11,28] The local symmetry of the octahedral interstitial site is that of the point group S_6. The octahedral site is shown schematically in Fig. 1. It is formed by the six nearest-neighbor C_{60} molecules, whose centers lie on the three mutually orthogonal axes, at the distance of 13.27 bohrs from the center of the octahedral cavity. The C_{60} molecules are taken to be static (i.e., their centers and orientations fixed) and internally rigid.

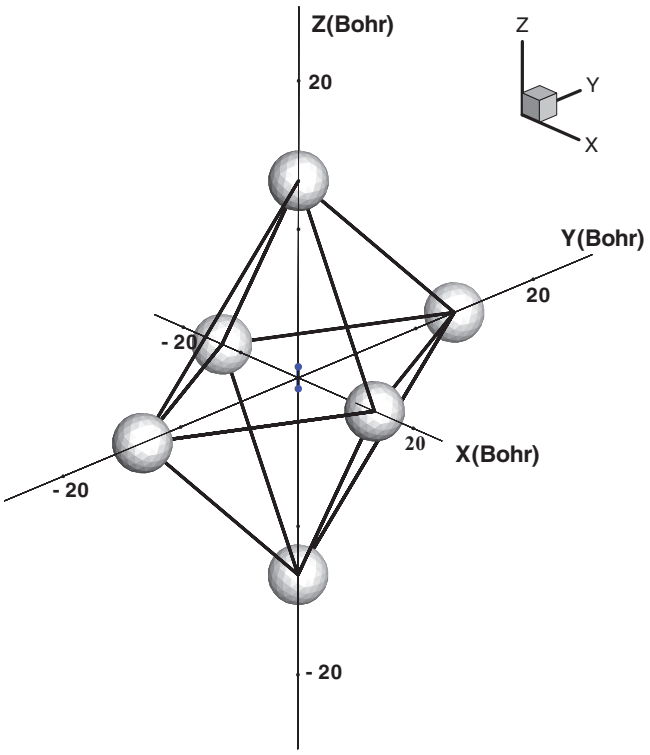

FIG. 1. A schematic depiction of the octahedral interstitial site of solid C_{60}, inside which an H_2 molecule is trapped. Black circles represent the C_{60} molecules.

The bond length of H_2 is held fixed. This is justified by the fact that the intramolecular stretch frequency of H_2, $\sim$4100 cm^{-1}, is much higher than those of the intermolecular TR modes. Therefore, the H_2 stretch vibration is coupled very weakly to the TR motions, and can be treated as frozen. The position of the H_2 molecule within the site is defined completely by the five coordinates $\mathbf{q} = (x, y, z, \theta, \phi)$; x, y, and z are the Cartesian coordinates of the center of mass (cm) of H_2, while the two polar angles θ and ϕ specify the orientation of the molecule. As in our previous investigations of H_2 in fullerenes,[20,22–24] the intermolecular 5D PES of H_2 in the octahedral site, $V(\mathbf{q})$, is constructed by summing over the pairwise interactions of each of the two H atoms with every one of the 360 C atoms of the six C_{60} molecules forming the site:

$$V(\mathbf{q}) = \sum_{i \in H_2} \sum_{j \in C_{60}} V_{\mathrm{H-C}}(r_{ij}), \tag{1}$$

where $V_{\mathrm{H-C}}$ is the H–C atom-atom pair potential to be specified shortly, and r_{ij} is the distance between the ith H atom and the jth C atom. For $V_{\mathrm{H-C}}$, we employ the potential:

$$V_{\mathrm{H-C}}(r) = Be^{-Cr} - A/r^6, \tag{2}$$

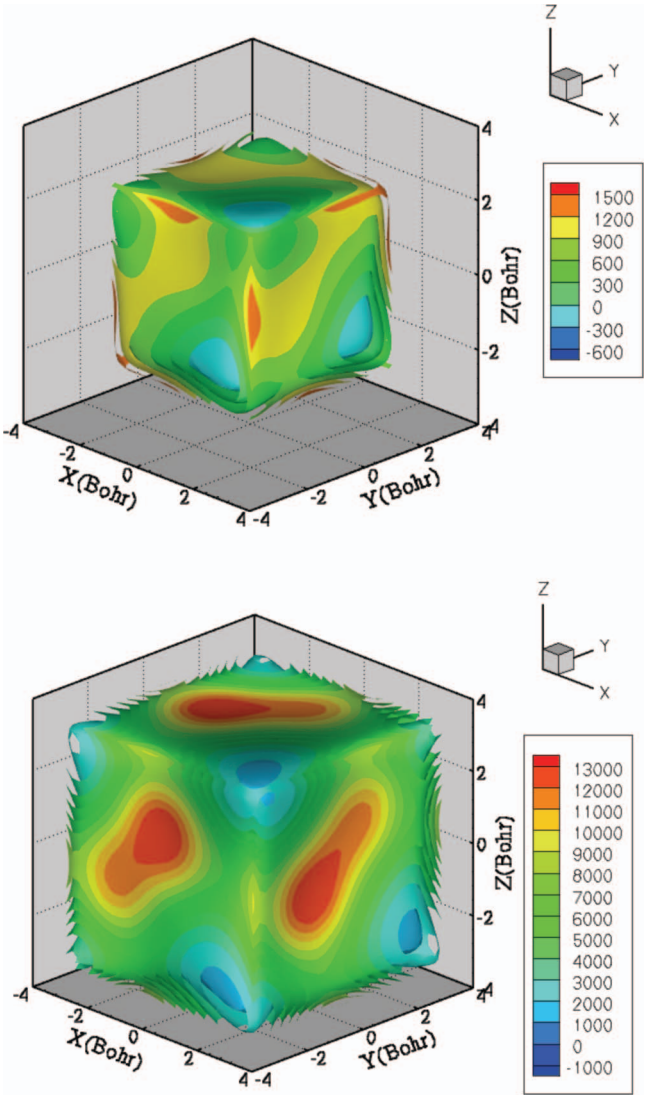

FIG. 2. The 3D isosurfaces of the 5D PES for H_2 inside the octahedral interstitial site. They are obtained by minimizing the PES with respect to the two angular coordinates of the H_2 molecule, at every position of its center of mass. In the bottom panel, the isosurfaces extend to much higher energies, in order to reveal features of the PES which are not visible in the top panel.

with $A = 5.941$ eV Å^6, $B = 678.2$ eV, and $C = 3.67$ Å^{-1}. This H–C potential has been used in several earlier studies of H_2 in solid C_{60}.[11,28,33] The 3D isosurface representation of the PES $V(\mathbf{q})$ is displayed in Fig. 2.

An issue which merits a comment here is that of the suitability of the three-site H_2–C pair potential,[22] developed by us earlier for H_2@C_{60}, for the present system. This H_2–C pair potential was optimized to reproduce quantitatively the IR spectra of H_2@C_{60}. In the early stages of this work, we utilized it also to construct another 5D PES of H_2 in the octahedral interstitial site. However, the results of the preliminary quantum 5D calculations on this PES were in significantly worse agreement with the experimental data than those obtained using the PES defined by Eqs. (1) and (2), and its use was discontinued. In the hindsight, this is not surprising. In the octahedral interstitial site, H_2 interacts with the exterior surfaces of the six C_{60} molecules forming the site. The π-electron density on the convex outer surface of C_{60} differs from that on the concave inner surface, and so does the interaction of H_2 with the exterior and the interior of the fullerene. Consequently, H_2–C pair potential optimized for H_2 inside C_{60} should not be expected to provide an accurate description of the H_2-host interaction in the octahedral interstitial site.

B. Calculation of the coupled translation-rotation eigenstates

The methodology for accurate and efficient calculation of the coupled 5D TR energy levels and wave functions of a hydrogen molecule inside nanoscale cavities, employed in this work, has been described in detail in Ref. 38. This approach has evolved in our group over a number of years, in the course of the theoretical investigations of the quantum TR dynamics of H_2 and its isotopologues entrapped in the cages of clathrate hydrates,[40–42] fullerenes C_{60} and C_{70},[20,22] and an open-cage derivative of C_{60} (ATOCF).[24]

For H_2 in the interstitial site formed by the six static C_{60} molecules, using the coordinates $\mathbf{q} = (x, y, z, \theta, \phi)$, the 5D Hamiltonian for its coupled TR motions can be written as[40]

$$H = -\frac{\hbar^2}{2m}\left(\frac{\partial^2}{\partial x^2} + \frac{\partial^2}{\partial y^2} + \frac{\partial^2}{\partial z^2}\right) + B\mathbf{j}^2 + V(\mathbf{q}). \qquad (3)$$

In Eq. (3), m is the mass of H_2 (2.016 amu), B and $\mathbf{j}^2$ denote the rotational constant and the angular momentum operator of the diatomic, respectively, and $V(\mathbf{q})$ is the 5D PES defined in Eqs. (1) and (2).

Comparison with the spectroscopic measurements on this system requires the computation of the TR eigenstates of the trapped H_2 in both the ground vibrational state $v = 0$ and the $v = 1$ vibrationally excited state. Using $B_e = 60.853$ cm^{-1} and $\alpha_e = 3.062$ cm^{-1} for the gas-phase H_2, and $B_v = B_e - \alpha_e(v + 1/2)$, one obtains $B_0 = 59.322$ cm^{-1} and $B_1 = 56.260$ cm^{-1}, for the $v = 0$ and $v = 1$ states, respectively. However, our calculations of the TR eigenstates of H_2 ($v = 1$) in the octahedral site of solid C_{60} utilized $B_1 = 55.6$ cm^{-1}, the value estimated from the IR spectroscopic measurements of this system.[31] This value is close to that for H_2 ($v = 1$) *inside* C_{60}, $B_1 = 55.404$ cm^{-1}, extracted from the IR spectra of H_2@C_{60}.[18] Both rotational constants are smaller than the gas-phase value; this is caused by the softening of the H_2 intramolecular potential due to the interaction with the host environment.

In the bound-state calculations,[38] the dimension of the sinc-discrete variable representation (DVR) basis was 20 for each of the three Cartesian coordinates x, y, and z, spanning the range -3.78 bohr $\leq \lambda \leq 3.78$ bohrs ($\lambda = x, y, z$). For p-H_2, the angular basis included even-j rotational functions up to $j_{max} = 6$, while the angular basis for o-H_2 included odd-j rotational functions up to $j_{max} = 7$. The cutoff parameter for the size of the intermediate 3D eigenvector basis was set to 400 lowest energy eigenvectors, resulting in the final 5D Hamiltonian matrices of dimension 11 200 for p-H_2 and 14 400 for o-H_2. These basis set parameters were chosen following extensive testing, assuring that the TR energy levels reported in this paper are converged to five significant figures or better. Diagonalization of the final 5D Hamiltonian matrices yields

the fully coupled TR energy levels and wave functions which are numerically exact for the 5D PES employed.

III. RESULTS AND DISCUSSION

A. Translation-rotation energy levels of *p*-H_2

The first 39 excited TR energy levels of *p*-H_2 ($v = 0$) in the octahedral site of solid C_{60}, from our quantum 5D calculations, are given in Table I, together with their degeneracies. They encompass all $j = 0$ TR levels with up to four quanta of translational excitation; in this energy range are also the $j = 2$ TR levels with zero, one, and two quanta in the translational modes. The global minimum of the PES is at -926.93 cm^{-1} while the TR ground-state energy E_0 is equal to -769.48 cm^{-1} for *p*-H_2 ($v = 0$); therefore, the zero-point energy (ZPE) of the TR motions is 157.45 cm^{-1}. To put this in perspective, the ZPE of the TR motions of *p*-H_2 *inside* C_{60} is 241.55 cm^{-1}.[22] This value was calculated for H_2 in the $v = 1$ state, but the excitation of the H_2 stretch mode has a very small effect on the TR ZPE. The fact that the TR ZPE for H_2 in the octahedral site of solid C_{60} is substantially smaller than that of H_2 inside the C_{60} molecule implies that H_2 is confined more tightly in the latter.

TABLE I. TR energy levels of *p*-H_2 ($v = 0$) molecule inside the octahedral cavity of solid C_{60}. The excitation energies ΔE^{5D} (in cm^{-1}) from the quantum 5D calculations in this work are relative to the TR ground state $E_0 = -769.48$ cm^{-1}; g denotes the degeneracy of the levels. The quantum numbers n and l are those of the 3D isotropic harmonic oscillator. The quantum 3D translational ($j = 0$) energy levels ΔE^{3D} (in cm^{-1}) are from Ref. 33.

i	ΔE^{5D}	g	n	l	j	ΔE^{3D} (Ref. 33)	S_6
1	105.88	1	**1**	1	0	106.14	A_u
2	116.37	2	**1**	1	0	116.71	E_u
3	215.59	1	**2**	2	0	215.27	A_g
4	221.26	2	**2**	2	0	221.72	E_g
5	247.48	1	**2**	0	0	245.27	A_g
6	252.87	2	**2**	2	0	253.18	E_g
7	324.04	1	**3**	3	0	323.43	A_u
8	342.69	2	**3**	3	0	341.98	E_u
9	345.14	1	**3**	1	0	342.14	A_u
10	351.79	1	**0**	0	**2**	⋯	A_g
11	353.72	2	**0**	0	**2**	⋯	E_g
12	358.82	2	**3**	3	0	358.11	E_u
13	358.88	2	**0**	0	**2**	⋯	E_g
14	368.38	1	**3**	3	0	369.64	A_u
15	402.04	2	**3**	1	0	398.12	E_u
16	404.72	1	**3**	3	0	402.07	A_u
17	444.14	1	**4**	4	0	⋯	A_g
18	450.55	1	**1**	1	**2**	⋯	A_u
19	455.07	2	**1**	1	**2**	⋯	E_u
20	456.37	2	**4**	4	0	⋯	E_g
21	457.06	2	**1**	1	**2**	⋯	E_u
22	464.22	1	**1**	1	**2**	⋯	A_u
23	469.16	1	**1**	1	**2**	⋯	A_u
24	470.87	2	**4**	2	0	⋯	E_g
25	470.94	1	**4**	0	0	⋯	A_g
26	472.15	2	**1**	1	**2**	⋯	E_u
27	475.43	2	**1**	1	**2**	⋯	E_u
28	480.22	1	**1**	1	**2**	⋯	A_u
29	488.35	2	**1**	1	**2**	⋯	E_u
30	495.08	1	**1**	1	**2**	⋯	A_u
31	502.62	1	**4**	2	0	⋯	A_g
32	505.62	1	**4**	4	0	⋯	A_g
33	506.24	2	**4**	4	0	⋯	E_g
34	509.10	2	**4**	4	0	⋯	E_g
35	559.83	1	**2**	2	**2**	⋯	A_g
36	564.61	2	**2**	2	**2**	⋯	E_g
37	566.44	2	**2**	2	**2**	⋯	E_g
38	567.35	2	**4**	2	0	⋯	E_g
39	567.84	1	**4**	4	0	⋯	A_g

Useful information regarding the nature of the translational excitations of the guest H_2 molecule is provided by the 3D reduced probability density (RPD) $\rho_i(x, y, z)$ in the translational (Cartesian) coordinates:[40]

$$\rho_i(x, y, z) = \int \psi_i^*(x, y, z, \theta, \phi)\psi_i(x, y, z, \theta, \phi) \sin\theta d\theta d\phi, \tag{4}$$

where $\psi_i(x, y, z, \theta, \phi)$ is the ith T-R eigenfunction of the encapsulated *p*-H_2 or *o*-H_2. Fig. 3 shows the RPDs of the three $j = 0$ states ($i = 1, 2$ in Table I) having one quantum of translational excitation, while Fig. 4 displays the RPDs of the six $j = 0$ states ($i = 3$–6 in Table I) with two quanta of translational excitation. Fig. 4 in particular suggests strongly that the quantum numbers most appropriate for the assignment of the translationally excited TR eigenstates in the octahedral site are those of the 3D isotropic harmonic oscillator (HO), the principal quantum number n and the orbital angular momentum quantum number l, whose allowed values are n, $n - 2, \ldots 1$ or 0, for odd or even n, respectively.[43] When the possible values of m, $-l \le m \le l$, are taken into account, the degree of degeneracy of the energy levels of the isotropic 3D HO is $\frac{1}{2}(n + 1)(n + 2)$, e.g., 3 for $n = 1$, 6 for $n = 2$, 10 for $n = 3$, and 15 for $n = 4$.

The five $n = 2$ TR levels $i = 3$, 4, 6, whose RPDs in Fig. 4 resemble closely the d ($l = 2$) orbitals of the hydrogen atom, are clearly the members of the $n = 2$, $l = 2$ quintuplet, and the sixth level $i = 5$, with an almost spherical RPD, is the single $n = 2$, $l = 0$ state. Along the same lines, within the $j = 0$, $n = 3$ manifold, seven states, $i = 7$, 8, 12, 14, and 16, can be assigned as $n = 3$, $l = 3$, while three states, $i = 9$ and 15, are assigned as $n = 3$, $l = 1$. The fact that energies of the TR levels depend not only on n, as they do in the 3D isotopic HO,[43] but also on l, is evidence of the anharmonicity of the PES, which we observed also in our previous studies of H_2 inside C_{60}[20–22] and the large cage of the structure II clathrate hydrate.[42]

However, the five $n = 2$, $l = 2$ states are not degenerate, and neither are the seven states with $n = 3$, $l = 3$ nor the three with $n = 3$, $l = 1$. In fact, Table I shows that the TR levels exhibit at most double degeneracy, starting with the translational fundamental whose $n = 1$, $l = 1$ triplet is split into a nondegenerate ($i = 1$) and a doubly degenerate level ($i = 2$). This large reduction of degeneracy must be due to something other than the anharmonicity of the potential. The most obvious assumption is that it is caused by the crystal field of the interstitial site, i.e., the symmetry of the potential felt by the H_2, which is S_6 in this case. Our earlier theoretical studies

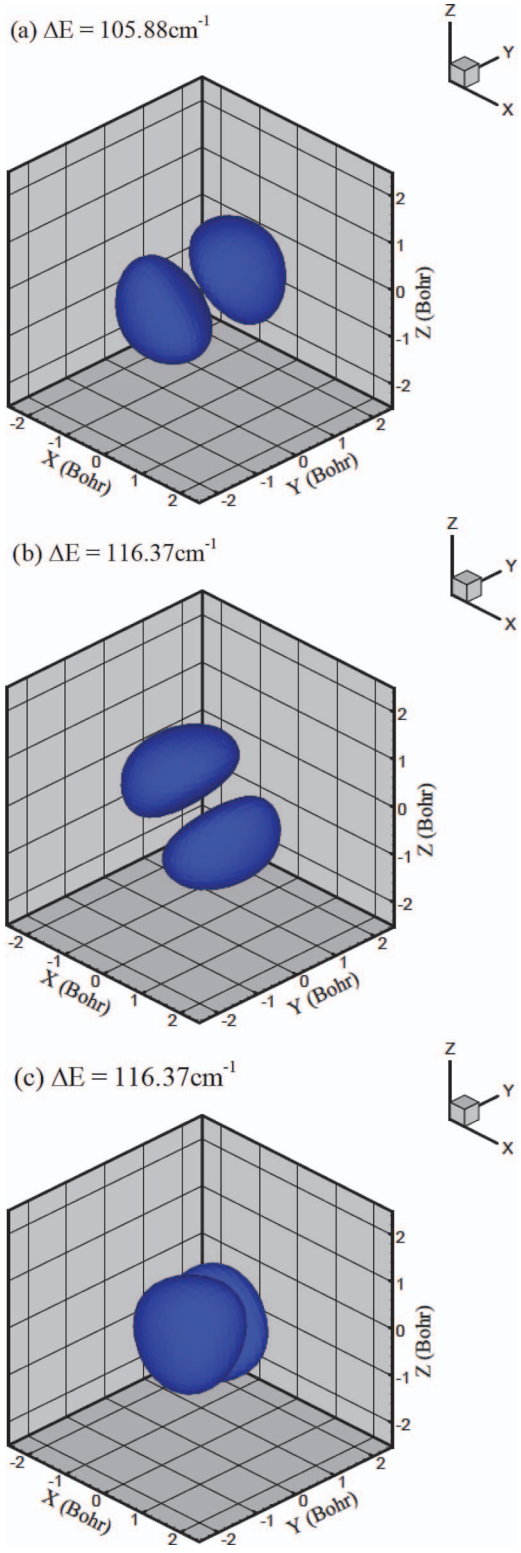

FIG. 3. The 3D isosurfaces of the reduced probability densities in the translational (Cartesian) coordinates of the three $n = 1$, $l = 1$ states of p-H_2 ($v = 0$) in the octahedral interstitial site. These $j = 0$ states have one quantum of excitation in the translational modes. The excitation energies ΔE are relative to the ground state.

have identified crystal-field induced splittings of degenerate translationally excited states of H_2 in C_{60} (I_h) for $n \geq 3$,[20] $C_{70}(D_{5h})$,[22] and the large cage of the sII clathrate hydrate (T_d, framework O atoms only).[42]

Yildirim and Harris have provided a beautiful in-depth analysis of the effects of the S_6 symmetry on the degeneracies of the TR energy levels of H_2 in the octahedral site of solid C_{60}.[33] For the $j = 0$ manifold, they investigated by means of the perturbation theory what happens to the $n = 1$–3 energy levels of the 3D isotropic HO as its symmetry is gradually lowered, first by the anharmonicity, and then by the external potentials having (a) O_h symmetry appropriate for orientationally disordered solid C_{60}, and finally (b) S_6 symmetry which applies to the orientationally ordered ($Pa\bar{3}$) phase of the solid C_{60}; see Fig. 1 of Ref. 33. Their perturbative model, despite its simplicity, incorporates the essential features of the full problem. The pattern of degeneracies that it yields for the potential of S_6 symmetry, with the nondegenerate levels belonging to the 1D A_u and A_g irreducible representations (irreps), and the doubly degenerate levels associated with the 2D E_u and E_g irreps, matches that from our quantum 5D calculations in Table I, allowing a straightforward symmetry assignments of the latter. In the $j = 0$, $n = 3$ manifold, the energy ordering of our nondegenerate and degenerate quantum 5D levels is generally reversed relative to that from the model calculations[33] showing that, not surprisingly, the model is not sufficiently quantitative to account for such fine details.

In addition to the perturbation treatment above, Yildirim and Harris have also performed a quantum 3D calculation of the purely translational ($j = 0$) energy levels of H_2 with $n = 1$–3 in the octahedral site, by treating H_2 as a spherical particle on a radially anisotropic 3D PES with S_6 symmetry, which depends only on the position of the cm of H_2.[33] Their PES was obtained by averaging the 5D PES employed in this work, specified by Eqs. (1) and (2), over the angular coordinates of H_2. The ($j = 0$) energy levels from their 3D calculation, for $n = 1$–3, are also shown in Table I. In most cases, they differ by less than 1 cm^{-1} from the corresponding energy levels obtained in the 5D calculations. The differences are larger in several instances. According to the 3D calculations, the levels $i = 8$ and $i = 9$ are nearly degenerate, separated by only 0.16 cm^{-1}, while in the 5D calculations their energies differ by 2.45 cm^{-1}. In addition, the energies of the levels $i = 5$, 15, and 16 from the 5D calculations are 2.21, 3.92, and 2.65 cm^{-1}, respectively, higher than those obtained in the 3D calculations of Yildirim and Harris.[33] Very good overall agreement between the 3D and 5D quantum calculations implies that treating H_2 as a spherical particle is a good approximation for calculating its translational ($j = 0$) energy levels in the octahedral site of solid C_{60}.

Also shown in Table I are the quantum 5D TR eigenstates belonging to the $j = 2$ manifold. The five $j = 2$, $n = 0$ states are interspersed among the $n = 3$ states with $j = 0$. All 15 $j = 2$, $n = 1$ states lie entirely in the energy range spanned by the $n = 4$ states in the ground rotational state $j = 0$, together with five (out of 30) $j = 2$, $n = 2$ TR eigenstates. The $j = 2$ manifold, with or without translational excitations, was not treated at all by Yildirim and Harris.[33] It is not clear how accurate would be their computational approach, in which every n, j manifold is treated separately, as decoupled from others, in the case when several manifolds overlap.

The five $j = 2$ energy levels in the ground translational state $n = 0$, $i = 10$, 11, and 13, are split in a 1:2:2 degeneracy

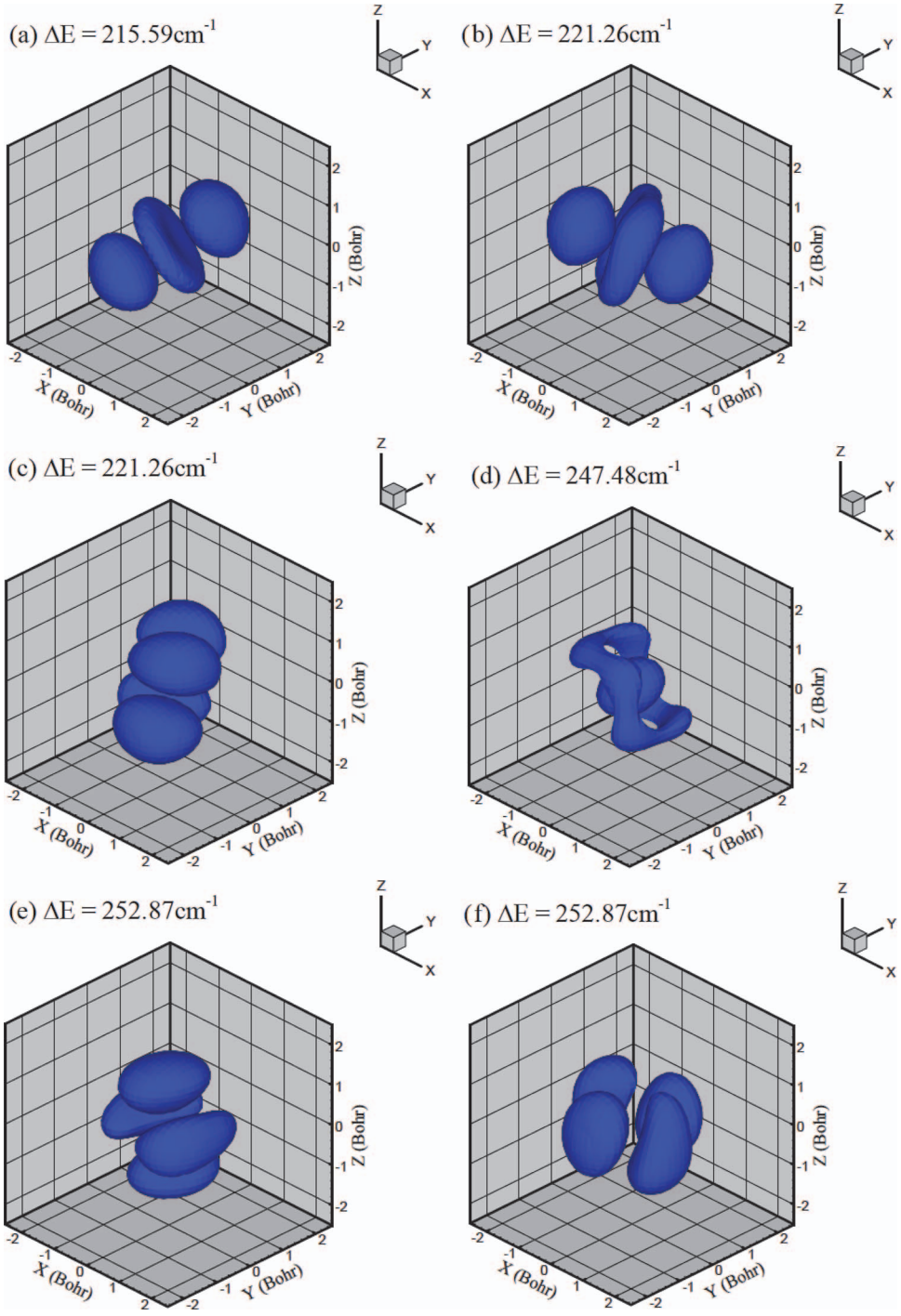

FIG. 4. The 3D isosurfaces of the reduced probability densities (RPDs) in the translational (Cartesian) coordinates of the six $n = 2$ states of p-H_2 ($v = 0$) in the octahedral interstitial site. These $j = 0$ states have two quanta of excitation in the translational modes. The panels (a)–(c), (e), and (f) show the RPDs of the five $n = 2$, $l = 2$ states, while panel (d) shows the RPD of the $n = 2$, $l = 0$ state. The excitation energies ΔE are relative to the ground state.

pattern by the angular anisotropy (crystal-field effects) of the octahedral site. The splittings between the three components of the quintuplet are highly uneven. The nondegenerate and the closest doubly degenerate $j = 2$ levels, $i = 10$ and 11, are split by only 1.93 cm^{-1}, while the second degenerate $j = 2$ level, $i = 13$, lies 5.16 cm^{-1} above $i = 11$.

Table II compares the energies of $j = 2$ (and $j = 1$) rotational levels from the quantum 5D calculations (for the ground translational state) with those from the purely rotational quantum 2D bound-state calculation on the same PES in which the cm of H_2 ($v = 0$) is fixed at the center of the octahedral site. Also shown are the overall splittings Δ, which for $j = 2$ are defined as the energy difference between the highest energy doubly degenerate component and the nondegenerate component of the quintuplet. The overall splitting of the quantum 5D $j = 2$ levels (the energy difference between the levels $i = 10$ and $i = 13$ in Table I), 7.09 cm^{-1}, is more than a factor of two greater than that from the quantum 2D calculations, 3.27 cm^{-1}. This demonstrates the importance of including the vibrational averaging over ground-state wave function for

TABLE II. Energies (in cm^{-1}) of the $j = 1$ and $j = 2$ rotational levels, together with their respective splittings Δ (in cm^{-1}), from the quantum 5D calculations (for the ground translational state) and purely rotational quantum 2D calculations, for H_2 ($v = 0$) molecule inside the octahedral cavity of solid C_{60} in this work. g denotes the degeneracy of the level. For $j = 1$, Δ is the energy difference between the doubly degenerate and nondegenerate components of the triplet. For $j = 2$, Δ is the energy difference between the highest energy doubly degenerate component and the nondegenerate component of the quintuplet.

	g	5D	2D
$j = 1$	1	115.61	116.81
	2	119.26	119.29
		$\Delta = 3.65$	$\Delta = 2.48$
$j = 2$	1	351.79	352.55
	2	353.72	353.52
	2	358.88	355.82
		$\Delta = 7.09$	$\Delta = 3.27$

obtaining the accurate value of the splitting of the $j = 2$ manifold. The larger value of the splitting obtained from the 5D calculations can be readily explained: the ground-state wave function of H_2 is significantly delocalized, and samples the regions of the PES closer to the site walls, where the angular anisotropy is stronger than in the vicinity of the center of the site, at which the H_2 is fixed in the quantum 2D calculations.

B. Translation-rotation energy levels of *o*-H_2

When both the translational and rotational degrees of freedom of a nanoconfined H_2 molecule are excited, as in the $j = 1, n = 1$ manifold of the caged *o*-H_2, the TR coupling lifts in part the degeneracy of the manifold. The remaining degeneracies are reduced further by the crystal-field effects of the environment. Therefore, the final pattern of the level degeneracies is the result of the interplay between the TR coupling and the symmetry of the nanocavity in which H_2 is entrapped.

For H_2 *inside* the highly symmetric (icosahedral) fullerene C_{60}, our quantum 5D calculations of the TR eigenstates and their analysis[20–22] have shown that the orbital angular momentum $\boldsymbol{l}$ and the rotational angular momentum $\boldsymbol{j}$ couple vectorially to give the total angular momentum $\boldsymbol{\lambda} = \mathbf{l} + \mathbf{j}$ having the values $\lambda = l + j, l + j - 1, \ldots, |l - j|$, and the degeneracy of $2\lambda + 1$. The eigenstates with the same quantum numbers n and j (both nonzero) split into as many distinct levels as there are different values of λ, each having the degeneracy of $2\lambda + 1$. Thus, the nine $j = 1$, $n = 1$ eigenstates of *o*-H_2@C_{60} are split into three levels corresponding to $\lambda = 1$, 2, and 0, respectively (with the degeneracies of 3, 5, and 1). Our predictions were subsequently verified by the IR[17] and INS[16] spectroscopic measurements of H_2@C_{60}. As mentioned earlier, the crystal field of the icosahedral (I_h) cavity of C_{60} induces additional fine splittings of the TR eigenstates with $\lambda \geq 3$.[20] These splittings do not exceed 0.5–1 cm^{-1}, reflecting the very weak icosahedral "corrugation" of the C_{60} cavity.[20–22]

In the orientationally ordered $Pa\bar{3}$ structure of solid C_{60}, the octahedral interstitial site has the much lower symmetry of the S_6 point group. This results in the TR energy level structure which is completely different from that of H_2@C_{60}. This is evident from Table III, which gives the first 20 TR energy levels of *o*-H_2 ($v = 0$) in the octahedral site of solid C_{60}, from the quantum 5D calculations, and their degeneracies. Included in it are the $j = 1$ TR levels with zero, one, and two quanta ($n = 0$–2) of translational excitation. Just as the $j = 0$ levels shown in Table I, the $j = 1$ levels are at most doubly degenerate. The nine TR states with $j = 1$, $n = 1$ are split into six levels, while the 18 $j = 1$, $n = 2$ TR states appear as 12 distinct levels. The energy differences between them, ranging from about 2 to 14 cm^{-1}, are much larger than the crystal-field induced level splittings in H_2@C_{60}. Yildirim and Harris[33] have performed a detailed group-theoretical analysis of the $j = 1$, $n = 1$ manifold of *o*-H_2 in the octahedral site having S_6 symmetry, and the symmetry labels of our quantum 5D levels are based on their results.

TABLE III. TR energy levels of *o*-H_2 ($v = 0$) molecule inside the octahedral cavity of solid C_{60}, with zero, one, and two quanta of translational excitation ($n = 0$, 1, 2), and $j = 1$. The excitation energies ΔE^{5D} (in cm^{-1}) from the quantum 5D calculations in this work are relative to the TR ground state of *p*-H_2 ($v = 0$), $E_0 = -769.48$ cm^{-1}; g denotes the degeneracy of the levels. The quantum numbers n and l are those of the 3D isotropic harmonic oscillator. The $n = 1$, $j = 1$ levels denoted $\Delta E^{5D}_{j=1}$, from $i = 3$ to $i = 8$, are obtained by subtracting $2B_0 = 118.644$ cm^{-1} from the corresponding energy levels in the column under ΔE^{5D}. This is done to enable comparison with the energy levels in the column under $\Delta E_{j=1}$ (in cm^{-1}), which are from the approximate quantum calculations in Ref. 33 and have the same zero-of-energy. For additional explanation, see the text.

i	ΔE^{5D}	$\Delta E^{5D}_{j=1}$	g	n	l	$\Delta E_{j=1}$ (Ref. 33)	S_6
1	115.61	⋯	1	**0**	0	⋯	A_u
2	119.26	⋯	2	**0**	0	⋯	E_u
3	217.82	99.18	1	**1**	1	101.55	A_g
4	219.41	100.77	2	**1**	1	103.40	E_g
5	224.70	106.06	2	**1**	1	108.64	E_g
6	230.63	111.99	1	**1**	1	114.53	A_g
7	243.60	124.96	1	**1**	1	127.03	A_g
8	250.71	132.07	2	**1**	1	133.89	E_g
9	318.57	⋯	1	**2**	2	⋯	A_u
10	323.74	⋯	2	**2**	2	⋯	E_u
11	337.41	⋯	2	**2**	2	⋯	E_u
12	338.29	⋯	1	**2**	2	⋯	A_u
13	348.18	⋯	2	**2**	2	⋯	E_u
14	352.31	⋯	1	**2**	2	⋯	A_u
15	354.97	⋯	1	**2**	0	⋯	A_u
16	355.33	⋯	2	**2**	0	⋯	E_u
17	361.84	⋯	1	**2**	2	⋯	A_u
18	364.93	⋯	2	**2**	2	⋯	E_u
19	401.72	⋯	2	**2**	2	⋯	E_u
20	404.79	⋯	1	**2**	2	⋯	A_u

Also shown in Table III are the TR energy levels which Yildirim and Harris obtained by diagonalizing a 9×9 matrix for the $j = 1$, $n = 1$ manifold, using the same PES.[33] This reduced-dimension approach assumes (a) no coupling between the states with different j values, and (b) that for a given j, translational states with a different number of translational quanta n can be treated separately. Hence, their calculation does not include the $j = 1$, $n = 0$ states (nor those with $j = 1$, $n = 2$). Therefore, we had to subtract $2B_0 = 118.644$ cm^{-1} from our fully coupled quantum 5D $j = 1$,

TABLE IV. Overall splittings Δ_v (in cm^{-1}) of the TR energy levels of p-H_2 ($j = 0$) for $n = 1$–4, and of o-H_2 ($j = 1$) for $n = 1$–3, from the quantum 5D calculations in this work for the entrapped H_2 ($v = 0$) molecule. The splittings represent the energy differences between the highest and lowest energy states within a given n, j manifold. The level energies are relative to the TR ground state of p-H_2 ($v = 0$), $E_0 = -769.48$ cm^{-1}.

p-H_2 ($j = 0$)			o-H_2 ($j = 1$)		
n	Δ_v	Energy range (cm^{-1})	n	Δ_v	Energy range (cm^{-1})
$n = 1$	10.49	105.9–116.4			
$n = 2$	37.28	215.6–252.9	$n = 1$	32.89	217.8–250.7
$n = 3$	80.68	324.0–404.7	$n = 2$	86.22	318.6–404.8
$n = 4$	123.43	441.4–567.8	$n = 3$	142.43	432.9–575.3

$n = 1$ energy levels in Table III, in order to make the comparison with the levels of Yildirim and Harris, for which this is the zero-of-energy.[33] Inspection of Table III shows that the two sets of $j = 1$, $n = 1$ energy levels differ by no more than 3 cm^{-1}. Yildirim and Harris[33] did not consider the $j = 1$, $n = 2$ manifold, so no comparison is possible with our 5D results.

The $j = 1$ triplet for the ground translational state exhibits a 1:2 pattern, i.e., it is split into a single state and a pair of degenerate states, separated by 3.65 cm^{-1} in the quantum 5D calculations. As shown in Table II, the purely rotational quantum 2D bound-state calculation gives the significantly smaller splitting of 2.48 cm^{-1}, as in the case of the $j = 2$ quintuplet splitting discussed earlier. On the other hand, this 2D splitting is in excellent agreement with the value of 2.50 cm^{-1} obtained from the perturbative expression $\Delta = -(9/20\pi)^{1/2} V_{20}$, for $V_{20} = 6.61$ cm^{-1}, which also assumes that the cm of H_2 is fixed.[28] Interestingly, when the interaction potential is averaged over the range of the zero-point motions of the H_2 cm, using a Gaussian distribution,[28] the same expression yields the splitting of 3.63 cm^{-1}, in remarkable agreement with our quantum 5D result of 3.65 cm^{-1}. This consistency is satisfying, and once again confirms that taking into account the translational motions of the H_2 cm is essential for accurate calculations of the splittings of the $j = 1$ and $j = 2$ multiplets.

C. On the splittings and anharmonicity of the translation-rotation energy levels of *p*-H_2 and *o*-H_2

The TR energy level structure of H_2 in the octahedral interstitial site of solid C_{60}, presented in Tables I and III, is the result of an interplay between the anharmonicity of the guest-host interaction potential and the crystal field, i.e., the symmetry of the interstitial site. The combination of the two effects leads to the splitting of the TR energy levels within each j, n manifold, shown in Table IV for the $n = 1$–4 levels of p-H_2 ($j = 0$) and the $n = 1$–3 levels of o-H_2 ($j = 1$), from the quantum 5D calculations. For each j, n manifold, the overall splitting, denoted as Δ_v, is the energy difference between the highest and the lowest energy states in the manifold.

Table IV shows that for both p- and o-H_2, Δ_v increases rapidly with the number of translational quanta n. In the case of p-H_2, Δ_v equals 10.5 cm^{-1} for $n = 1$, 37.3 cm^{-1} for $n = 2$, 80.7 cm^{-1} for $n = 3$, and 124.4 cm^{-1} for $n = 4$. Thus, there is a nearly 12-fold increase in Δ_v for $n = 1$–4. The trend is very similar for o-H_2. This growth of Δ_v with increasing n is not surprising (although the magnitude may be), since one expects that both the anharmonicity of the PES, and its "corrugation," or the crystal field effects it causes, become larger in the higher energy regions of the PES, closer to the walls of the cavity.

But, inspection of Table IV reveals another less anticipated feature. Namely, in the range $n = 2$–4, the splitting Δ_v for a $j = 0$, n manifold of p-H_2 is very similar to that for a $j = 1$, $n - 1$ manifold of o-H_2. For example, $\Delta_v = 37.3$ cm^{-1} for the $n = 2$ manifold of p-H_2 ($j = 0$) can be compared to $\Delta_v = 32.9$ cm^{-1} for the $n = 1$ manifold of o-H_2 ($j = 1$). The same is true for all other manifolds shown in Table IV. To explain this observation, we note that for $n = 2$–4, a $j = 0$, n manifold of p-H_2 spans an almost identical energy range as a $j = 1$, $n - 1$ manifold of o-H_2. This is largely a consequence of the fact that the energy of the translational fundamental, 105.9–116.4 (Table I), happens to be close to that of the $j = 1$, $n = 0$ triplet, 115.6–119.3 cm^{-1} (Table III). From the results in Table IV, one can conclude that for this system, Δ_v depends primarily on the *total* energy of the levels in a manifold, regardless of whether it is partitioned as $j = 0$, n or $j = 1$, $n - 1$; lying in the same energy range, these TR eigenstates experience roughly the same potential anharmonicity and crystal field effects.

In closing, we discuss the energy separation between the neighboring translational excitations of p-H_2 ($j = 0$) having $n = 1$, 2, 3, and 4 (Table I). The issue is complicated by the large splittings of these manifolds. Therefore, we define the energy of the translational excitation with n quanta to be the midpoint of the corresponding manifold. Then, the energies of the ($j = 0$) transitional excitations with $n = 1$, 2, 3, and 4 are 111.1, 234.2, 364.4, and 505.9 cm^{-1}, respectively. The energy difference between the successive translational excitations slowly *increases* with n, from 123.1 cm^{-1} between $n = 1$ and $n = 2$, to 141.5 cm^{-1} between $n = 3$ and $n = 4$, evidence of the *negative* anharmonicity of the translational energy levels. Negative anharmonicity is common for H_2 in nanoscale cavities, as revealed by our earlier theoretical studies of H_2 in C_{60}[20,22] and C_{70}.[22]

D. Comparison with experiments

Experimental data regarding the rotational energy levels of H_2 in the octahedral site of solid C_{60}, and their splittings

TABLE V. Comparison of calculated and measured $j = 0 \rightarrow 1$ and $j = 0 \rightarrow 2$ rotational excitation energies (in cm^{-1}), and their respective splittings Δ (in cm^{-1}), for the ground translational state ($n = 0$). The theoretical results are from the quantum 5D calculations in this work. The numbers in the brackets denote the degeneracy of the level. For $j = 1$, Δ is the energy difference between the doubly degenerate and nondegenerate components of the triplet. For $j = 2$, Δ is the energy difference between the highest energy doubly degenerate component and the nondegenerate component of the quintuplet. For additional explanation, see the text.

Theory		Experiment
	$j = 1$	
	H_2 ($\nu = 0$)	
115.61 (1)[a]		112.1 (1)[b]
119.26 (2)[a]		117.8 (2)[b]
$\Delta = 3.65$[a]		$\Delta = 5.7$ (Ref. 28, INS); 5.45 (Ref. 11, NMR)
113.68 (1)[c]		
117.38 (2)[c]		
$\Delta = 3.69$[c]		
	$j = 2$	
	H_2 ($\nu = 1$)	
330.98 (1)		
333.12 (2)		328.6, 330.3, 334.3, 337.5
339.53 (2)		
$\Delta = 8.55$		$\Delta = 8.9$, IR

[a]The $j = 1$ results were calculated using the gas-phase values of the spectroscopic constants for H_2 ($\nu = 0$).
[b]From Ref. 28.
[c]The $j = 1$ results were calculated using the spectroscopic constants for H_2 ($\nu = 0$) in C_{60}, from Ref. 18.

due to the crystal-field effects, are rather limited. They are listed in Table V. Based on the INS measurements,[28] the energies of the singlet and doublet components of the $j = 1$ triplet for H_2 ($\nu = 0$) are 112.1 and 117.8 cm^{-1}, respectively. Our respective calculated values of 115.61 and 119.26 cm^{-1} are slightly larger. This is mainly due to the fact that the gas-phase value of the H_2 rotational constant was used in the calculations, which is larger than that for H_2 inside a carbon nanocavity, e.g., in C_{60} (Ref. 17). The calculated splitting of the $j = 1$ triplet, 3.65 cm^{-1}, is smaller than the experimental values, 5.7 cm^{-1} (INS[28]) and 5.45 cm^{-1} (NMR[11]).

Table V also shows the energies of nondegenerate and doubly degenerate sublevels of the $j = 1$ triplet for H_2 ($\nu = 0$) from the quantum 5D calculations performed using the spectroscopic parameters determined from the IR spectra of $H_2@C_{60}$ (Ref. 18), $B_0 = 58.378\ cm^{-1}$ and $D_e = 0.0483\ cm^{-1}$. Their values, 113.68 and 117.38 cm^{-1}, respectively, are in better agreement with the experimental results, in particular the energy of the doublet. This suggests that the rotational constants of H_2 in the octahedral site of solid C_{60} and inside C_{60} are very similar. The computed $j = 1$ splitting of 3.69 cm^{-1} is still smaller than the experimental result, about 5.7 cm^{-1} (Ref. 28), indicating that the PES employed slightly underestimates the angular anisotropy of the H_2 interaction with the octahedral cavity.

The only experimental information regarding the $j = 2$ multiplet comes from the IR spectroscopy of H_2 ($\nu = 1$) in solid C_{60}.[31] Very weak peaks at 328.6, 330.3, 334.3, and 337.5 cm^{-1}, listed in Table V, have been attributed to the $j = 2$, $n = 0$ manifold (in combination with the $Q(0)$ transition at 4104.3 cm^{-1}). Unfortunately, these weak peaks occur in the same frequency range as two vibrational modes of pure C_{60}; it is quite likely that at least one of them arises from an H_2-induced splitting of the C_{60} modes. The calculated sublevels of the $j = 2$ quintuplet in the ground translational state, which show the 1:2:2 degeneracy pattern, lie in the same energy range, but a more detailed assignment of the observed transitions is not possible at this time. The overall splitting of the $j = 2$ quintuplet from our calculations, 8.55 cm^{-1}, is in very good accord with the experimental value of 8.9 cm^{-1}.

There have been several attempts to determine experimentally the translational fundamental frequency of H_2 in the octahedral site of solid C_{60}. For H_2 ($\nu = 0$), neutron-scattering measurements showed peaks associated with the excitation of the translational modes of H_2 around 113 cm^{-1} (Ref. 28), and the NMR measurements have given an estimate of 105 cm^{-1} for the translational fundamental.[11] These estimates are consistent with our calculated values for the translational fundamental in Table I, which is split into a nondegenerate level at 105.88 cm^{-1} and a degenerate pair at 116.37 cm^{-1}. The IR spectra, which probe the dynamics of H_2 ($\nu = 1$), give the estimated value of 118 cm^{-1} for the translational fundamental.[31] The small increase from the value of 113 cm^{-1} measured for H_2 ($\nu = 0$) was attributed to the slight stiffening of the intermolecular potential upon the intramolecular vibrational excitation of H_2.[31] This is supported by the quantum 5D energies calculated by us for the translational fundamental of H_2 ($\nu = 1$), 106.75 and 117.25 cm^{-1}, for the nondegenerate and doubly degenerate components, respectively.

The fine structure of the $S(0)$ transitions in the IR spectra measured for H_2 in solid C_{60} has been fitted to six transitions,[31] whose energies are given in Table VI; they are relative to the $Q(0)$ transition at 4104.3 cm^{-1}. These energies are associated with the $j = 2$, $n = 1$ manifold of H_2 ($\nu = 1$). Therefore, they can be compared with the $j = 2$, $n = 1$ TR energy levels of H_2 ($\nu = 1$) from our quantum 5D calculations, also shown in Table VI. The calculated and measured TR levels lie in the same energy range. However, theory predicts ten energy levels with $j = 2$, $n = 1$, while only six have been resolved experimentally. A more definitive interpretation and assignment will require higher resolution IR spectra on one hand, and computed intensities of the spectroscopic transitions on the other.

E. Dependence of the translation-rotation energy levels on the setting angle

Theoretical studies of H_2 in solid C_{60}, and their comparison with experiments, are complicated by a subtle issue that we have not discussed so far. It is known that the low-temperature $Pa\bar{3}$ phase is characterized by a four-C_{60} unit cell. Starting from the "standard orientation" the four molecules at (0,0,0), (1/2,1/2,0), (1/2,0,1/2), (0,1/2,1/2) are rotated by the same angle, Γ, about local threefold axes $\langle 111 \rangle$, $\langle 1\bar{1}\bar{1} \rangle$, $\langle \bar{1}1\bar{1} \rangle$, $\langle \bar{1}\bar{1}1 \rangle$, respectively.[44] However, the actual value of the rotation angle Γ, which is governed by the intermolecular interactions between the C_{60} molecules and is not fixed by symmetry, is still uncertain. Attempts to determine Γ, which

TABLE VI. Comparison of calculated and measured $j = 2$, $n = 1$ TR energy levels of p-H_2 ($v = 1$). The excitation energies ΔE^{5D} from the quantum 5D calculations in this work are relative to the TR ground state of p-H_2 ($v = 1$), $E_0 = -766.21$ cm^{-1}; g denotes the degeneracy of the calculated levels. For all the levels shown, $l = 1$. These energy levels are interspersed with the levels belonging to the $j = 0$ manifold, which are not shown. The experimental results are from the IR spectra in Ref. 31. All energies are in cm^{-1}. For additional explanation, see the text.

i	ΔE^{5D}	g	Experiment
17	430.11	1	
18	434.95	2	
19	437.83	2	
20	445.83	1	439.7, 443.7, 448.7
22	449.78	1	450.7, 452.7, 461.7
23	453.07	2	
24	456.14	2	
26	461.24	1	
28	472.88	2	
30	479.80	1	

has become known as the setting angle,[45] have focused on optimizing fits to both neutron and x-ray diffraction data. These have yielded a range of values, 26°,[26] 25°–29°,[46] 22.5°,[47] 24°,[48] and 26.5°.[49] The situation is further complicated by the existence of the so called minority phase, which undergoes a different rotation angle, has a ≈11 meV higher energy than the ground state configuration, and is believed to be occupied by ≈1/6 of the molecules upon cooling below a glassy transition at ≈90 K.[44] Theoretical studies to date have assumed that the presence of C_{60} molecules with the minor orientation does not affect significantly the local crystal field of the interstitial site,[11,28,33] and we have adopted the same approach in this work.

To explore the sensitivity of the crystal-filed induced splitting of the $j = 1$ triplet on the value of the setting angle Γ, the cm of H_2 was fixed at the center of the octahedral cavity, and the resulting 2D PES expanded in terms of spherical harmonics:

$$V(\theta, \phi) = V_0 + \sum_{L=1}^{\infty} \sum_{m=-L}^{m=L} V_{Lm} Y_L^m(\theta, \phi), \qquad (5)$$

for the entire range of Γ. Of particular interest is the coefficient V_{20}, since in the perturbative approach[28] it determines both the magnitude of the $j =$ triplet splitting Δ, given as $\Delta = -(9/20\pi)^{1/2} V_{20}$, and the ordering of the nondegenerate and doubly degenerate $j = 1$ sublevels. The degeneracy pattern is 2:1 for positive, and 1:2 for negative values of V_{20}. The dependence of V_{20} on Γ is shown in Fig. 5. It is evident that V_{20}, and hence the rotational level splitting, varies strongly with Γ. In particular, there is a large change of V_{20} in the rather narrow range of the experimentally established possible values of Γ, 22°–29°.

This finding prompted us to perform quantum 5D calculations of the TR levels of the guest H_2 for several values of the setting angle. The dependence of the quantum 5D $j = 1$ and $j = 2$ rotational levels ($n = 0$), and their splittings, and of the translational fundamental and its splitting, on the setting angle Γ, is presented in Table VII. While the absolute

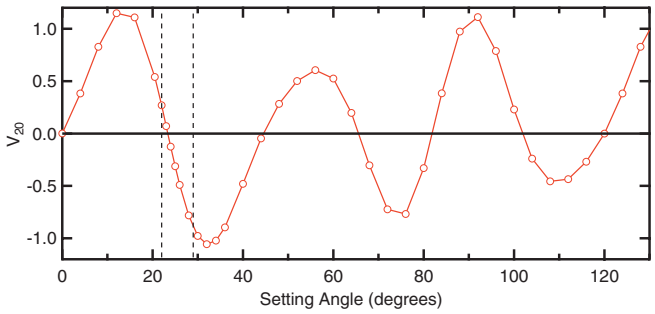

FIG. 5. Coefficient V_{20} in Eq. (5) as a function of the setting angle Γ. The dashed vertical lines mark the experimentally established region of possible values of Γ.

values of the energy levels only change by a few percent for different Γ values, their splittings vary quite drastically. This is most noticeable for the $j = 1$, $n = 0$ and $j = 0$, $n = 1$ levels where the splitting increases by more than a factor of four on going from a setting angle of 24.5°–28°.

This illustrates how important, indeed essential, it is to consider and define the setting angle Γ in any theoretical modeling of this system. It is therefore unfortunate that previous theoretical studies either made no mention of the C_{60} rotation angle Γ being used,[33,34] or contain conflicting statements about the setting angle.[28] Our calculations are in best agreement with previous theoretical results of Yildirim and Harris[33] and FitzGerald *et al.*[28] for Γ equal to 28°. The agreement deteriorates sharply for other Γ values, which leads us to believe that Γ = 28° was used in these earlier studies. All the results presented in this paper have been calculated for this setting angle.

The strong dependence of the rotational as well translational level splittings on Γ suggests that this elusive quantity can be in principle determined by varying Γ to achieve the best match between the theoretical results and the correspond-

TABLE VII. Energies (in cm^{-1}) of the $j = 1$, $n = 0$ and $j = 2$, $n = 0$ rotational levels, and of the translational fundamental $j = 0$, $n = 1$, together with their respective splittings Δ (in cm^{-1}), as the function of the setting angle Γ. The results are from the quantum 5D calculations for H_2 ($v = 0$) molecule inside the octahedral cavity of solid C_{60} in this work. The numbers in the brackets denote the degeneracy of the level. The energies are relative to the TR ground-state energies of −777.24, −774.62, and −769.48 cm^{-1}, for Γ equal to 24.5°, 26°, and 28°, respectively. For $j = 1$, $n = 0$ and $j = 0$, $n = 1$, Δ is the energy difference between the doubly degenerate and nondegenerate components of the respective triplets. For $j = 2$, $n = 0$, Δ is the energy difference between the highest energy doubly degenerate component and the nondegenerate component of the quintuplet.

	24.5°	26°	28°
	117.49 (1)	116.61 (1)	115.61 (1)
j = 1, $n = 0$	118.32 (2)	118.76 (2)	119.26 (2)
	Δ = 0.83	Δ = 2.15	Δ = 3.65
	353.15 (1)	352.51 (1)	351.79 (1)
j = 2, $n = 0$	353.53 (2)	353.66 (2)	353.72 (2)
	358.02 (2)	358.35 (2)	358.88 (2)
	Δ = 4.90	Δ = 5.84	Δ = 7.09
	109.70 (1)	107.66 (1)	105.88 (1)
$j = 0$, **n = 1**	111.88 (2)	113.77 (2)	116.37 (2)
	Δ = 2.18	Δ = 6.11	Δ = 10.49

ing experimental data. However, this is predicated on having a highly accurate PES of H_2 in the octahedral site, so that Γ is the only parameter that remains to be optimized by fitting to the experimental level splittings. Otherwise, the optimal value of Γ determined in this way will be the one which to a greatest degree compensates for the inaccuracies of the PES, not necessarily the actual Γ value.

IV. SUMMARY

We have performed fully coupled quantum 5D calculations of the TR energy levels and wave functions of H_2 molecule, in the ground ($v = 0$) and the vibrationally excited ($v = 1$) states, trapped inside the octahedral interstitial site of solid C_{60} which has S_6 symmetry, using a pairwise additive intermolecular PES. These calculations have characterized the translational and rotational excitations of the guest H_2 for energies well beyond those considered in the earlier theoretical studies of this system, and have resulted in new insights regarding the TR energy level structure. Inspection of the reduced probability densities of the TR eigenstates shows that the translational excitations can be assigned in terms of the quantum numbers n and l of the 3D isotropic harmonic oscillator. For both p- and o-H_2, the overall splittings of the TR eigenstates having the same quantum number n was found to increase rapidly with n, while the translational excitations exhibit negative anharmonicity.

The TR energy levels obtained in the quantum 5D calculations have been compared with the spectroscopic data in the literature. The computed splitting of the $j = 1$ triplet is about 35% smaller than the measured value, indicating that the PES employed underestimates the angular anisotropy of the guest-host interaction. The calculated sublevels of the $j = 2$ quintuplet, exhibiting the 1:2:2 degeneracy pattern, fall in the energy range of the very weak peaks observed in the IR spectra of H_2 ($v = 1$) in solid C_{60}, which have been attributed to the $j = 2$, $n = 0$ manifold. The computed and measured overall splittings of the $j = 2$ quintuplet are in very good agreement. The calculated translational fundamental, split into a nondegenerate level and a degenerate pair, is compatible with the experimental estimates. The $j = 2$, $n = 1$ TR levels of H_2 ($v = 1$) from our quantum 5D calculations lie in the same range as the energies of the levels in the $j = 2$, $n = 1$ manifold extracted from the fine structure of the $S(0)$ transitions in the IR spectra of this system.

Finally, we have investigated the sensitivity of the calculated TR energy levels and their splittings to the so-called setting angle, which defines the orientation of the C_{60} molecules with respect to their local axes. Our calculations have revealed strong dependence of the crystal-field induced splittings of the $j = 1$ and $j = 2$ multiplets, and of the translational fundamental, on the setting angle, even in the narrow range of the possible values established experimentally. This implies that the setting angle must be carefully considered in any quantitative treatment of this system and comparison with spectroscopic measurements.

The quantum 5D TR wave functions obtained in the present work will be utilized to compute the INS spectra of H_2 in solid C_{60}, using our newly developed methodology for rigorous calculations of the INS spectra of a hydrogen molecule inside a nanocavity of an arbitrary shape.[37–39] Comparison with the experimental INS spectra will help in assessing the accuracy of the interaction potential of H_2 with the surrounding C_{60} molecules and its improvement.

ACKNOWLEDGMENTS

Partial support of this research by the National Science Foundation (NSF), through the Grant No. CHE-1112292 to Z.B. and Grant No. CHE-1111896 to S.F., is gratefully acknowledged. In addition, the work of Z.B. was supported in part at Technion by a fellowship from the Lady Davis Foundation.

[1] F. Schüth, Nature (London) **434**, 712 (2005).
[2] Y. H. Hu and E. Ruckenstein, Angew. Chem., Int. Ed. **45**, 2011 (2006).
[3] T. A. Strobel, K. C. Hester, C. A. Koh, A. K. Sum, and E. D. Sloan, Jr., Chem. Phys. Lett. **478**, 97 (2009).
[4] V. V. Struzhkin, B. Militzer, W. L. Mao, H. K. Mao, and R. J. Hemley, Chem. Rev. **107**, 4133 (2007).
[5] W. L. Mao, C. A. Koh, and E. D. Sloan, Phys. Today **60**(10), 42 (2007).
[6] N. L. Rosi, J. Eckert, M. Eddaoudi, D. T. Vodak, J. Kim, M. O'Keeffe, and O. M. Yaghi, Science **300**, 1127 (2003).
[7] L. J. Murray, M. Dinca, and J. R. Long, Chem. Soc. Rev. **38**, 1294 (2009).
[8] D. Zhao, D. Yuan, and H.-C. Zhou, Energy Environ. Sci. **1**, 222 (2008).
[9] M. Dinca and J. R. Long, Angew. Chem., Int. Ed. **47**, 6766 (2008).
[10] S. Mamone, J. Y.-C. Chen, R. Bhattacharyya, M. H. Levitt, R. G. Lawler, A. J. Horsewill, T. Rõõm, Z. Bačić, and N. J. Turro, Coord. Chem. Rev. **255**, 938 (2011).
[11] M. Tomaselli, Mol. Phys. **101**, 3029 (2003).
[12] M. Carravetta, O. G. Johannessen, M. H. Levitt, I. Heinmaa, R. Stern, A. Samoson, A. J. Horsewill, Y. Murata, and K. Komatsu, J. Chem. Phys. **124**, 104507 (2006).
[13] M. Carravetta, A. Danquigny, S. Mamone, F. Cuda, O. G. Johannessen, I. Heinmaa, K. Panesar, R. Stern, M. C. Grossel, A. J. Horsewill, A. Samoson, M. Murata, Y. Murata, K. Komatsu, and M. H. Levitt, Phys. Chem. Chem. Phys. **9**, 4879 (2007).
[14] A. J. Horsewill, K. S. Panesar, S. Rols, M. R. Johnson, Y. Murata, K. Komatsu, S. Mamone, A. Danquigny, F. Cuda, S. Maltsev, M. C. Grossel, M. Carravetta, and M. H. Levitt, Phys. Rev. Lett. **102**, 013001 (2009).
[15] A. J. Horsewill, S. Rols, M. R. Johnson, Y. Murata, M. Murata, K. Komatsu, M. Carravetta, S. Mamone, M. H. Levitt, J. Y.-C. Chen, J. A. Johnson, X. Lei, and N. J. Turro, Phys. Rev. B **82**, 081410(R) (2010).
[16] A. J. Horsewill, K. S. Panesar, S. Rols, J. Ollivier, M. R. Johnson, M. Carravetta, S. Mamone, M. H. Levitt, Y. Murata, K. Komatsu, J. Y.-C. Chen, J. A. Johnson, X. Lei, and N. J. Turro, Phys. Rev. B **85**, 205440 (2012).
[17] S. Mamone, M. Ge, D. Hüvonen, U. Nagel, A. Danquigny, F. Cuda, M. C. Grossel, Y. Murata, K. Komatsu, M. H. Levitt, T. Rõõm, and M. Carravetta, J. Chem. Phys. **130**, 081103 (2009).
[18] M. Ge, U. Nagel, D. Hüvonen, T. Rõõm, S. Mamone, M. H. Levitt, M. Carravetta, Y. Murata, K. Komatsu, J. Y.-C. Chen, and N. J. Turro, J. Chem. Phys. **134**, 054507 (2011).
[19] M. Ge, U. Nagel, D. Hüvonen, T. Rõõm, S. Mamone, M. H. Levitt, M. Carravetta, Y. Murata, K. Komatsu, X. Lei, and N. J. Turro, J. Chem. Phys. **135**, 114511 (2011).
[20] M. Xu, F. Sebastianelli, Z. Bačić, R. Lawler, and N. J. Turro, J. Chem. Phys. **128**, 011101 (2008).
[21] M. Xu, F. Sebastianelli, Z. Bačić, R. Lawler, and N. J. Turro, J. Chem. Phys. **129**, 064313 (2008).
[22] M. Xu, F. Sebastianelli, B. R. Gibbons, Z. Bačić, R. Lawler, and N. J. Turro, J. Chem. Phys. **130**, 224306 (2009).
[23] F. Sebastianelli, M. Xu, Z. Bačić, R. Lawler, and N. J. Turro, J. Am. Chem. Soc. **132**, 9826 (2010).
[24] S. Ye, M. Xu, Z. Bačić, R. Lawler, and N. J. Turro, J. Phys. Chem. A **114**, 9936 (2010).
[25] P. A. Heiney, J. E. Fischer, A. R. McGhie, W. J. Romanow, A. M. Denenstein, J. P. McCauley, Jr., A. B. Smith III, and D. E. Cox, Phys. Rev. Lett. **66**, 2911 (1991).

[26]R. Sachidanandam and A. B. Harris, Phys. Rev. Lett. **67**, 1467 (1991).
[27]W. I. F. David, R. M. Ibberson, J. C. Matthewman, K. Prassides, T. J. S. Dennis, J. P. Hare, H. W. Kroto, R. Taylor, and D. R. M. Walton, Nature (London) **353**, 147 (1991).
[28]S. A. FitzGerald, T. Yildirim, L. J. Santodonato, D. A. Neumann, J. R. D. Copley, J. J. Rush, and F. Trouw, Phys. Rev. B **60**, 6439 (1999).
[29]M. Tomaselli and B. H. Meier, J. Chem. Phys. **115**, 11017 (2001).
[30]S. A. FitzGerald, S. Forth, and M. Rinkoski, Phys. Rev. B **65**, 140302(R) (2002).
[31]S. A. FitzGerald, H. O. H. Churchill, P. M. Korngut, C. B. Simmons, and Y. E. Strangas, Phys. Rev. B **73**, 155409 (2006).
[32]K. A. Wiliams, B. K. Pradhan, P. C. Eklund, M. K. Kostov, and M. W. Cole, Phys. Rev. Lett. **88**, 165502 (2002).
[33]T. Yildirim and A. B. Harris, Phys. Rev. B **66**, 214301 (2002).
[34]R. M. Herman and J. C. Lewis, Phys. Rev. B **73**, 155408 (2006).
[35]B. P. Uberuaga, A. F. Voter, K. K. Sieber, and D. S. Sholl, Phys. Rev. Lett. **91**, 105901 (2003).
[36]A. V. Dolbin, V. B. Eselson, V. G. Gavrilko, V. G. Manzhelli, N. A. Vinnikov, and S. N. Popov, Low Temp. Phys. **38**, 962 (2012).
[37]M. Xu, L. Ulivi, M. Celli, D. Colognesi, and Z. Bačić, Phys. Rev. B **83**, 241403(R) (2011).
[38]M. Xu and Z. Bačić, Phys. Rev. B **84**, 195445 (2011).
[39]M. Xu, L. Ulivi, M. Celli, D. Colognesi, and Z. Bačić, Chem. Phys. Lett. **563**, 1 (2013).
[40]M. Xu, Y. Elmatad, F. Sebastianelli, J. W. Moskowitz, and Z. Bačić, J. Phys. Chem. B **110**, 24806 (2006).
[41]M. Xu, F. Sebastianelli, and Z. Bačić, J. Chem. Phys. **128**, 244715 (2008).
[42]M. Xu, F. Sebastianelli, and Z. Bačić, J. Phys. Chem. A **113**, 7601 (2009).
[43]L. D. Landau and E. M. Lifshitz, *Quantum Mechanics* (Pergamon Press, Oxford, 1977).
[44]M. S. Dresselhaus, G. Dresselhaus, and P. C. Eklund, *Science of Fullerenes and Carbon Nanotubes* (Academic Press, 1995).
[45]S. Savin, A. B. Harris, and T. Yildirim, Phys. Rev. B **55**, 14182 (1997).
[46]R. Z. Hu, T. Egami, F. Li, and J. S. Lannin, Phys. Rev. B **45**, 9517 (1992).
[47]W. I. F. David, R. M. Ibberson, T. J. S. Dennis, J. P. Hare, and K. Prassides, Europhys. Lett. **18**, 219 (1992).
[48]P. A. Heiney, J. Phys. Chem. Solids **53**, 1333 (1992).
[49]O. Blaschko, G. Krexner, C. Maier, and R. Karawatzki, Phys. Rev. B **56**, 2288 (1997).